

# Experimental, numerical and analytical studies of abrasive wear: correlation between wear mechanisms and friction coefficient

Salah Mezlini <sup>a,\*</sup>, M. Zidi <sup>a</sup>, H. Arfa <sup>a</sup>, Mohamed Ben Tkaya <sup>a</sup>, Philippe Kapsa <sup>b</sup>

<sup>a</sup> LGM, École nationale d'ingénieurs de Monastir, 5019 Monastir, Tunisia

<sup>b</sup> LTDS, UMR CNRS 5513, École centrale de Lyon, 36 avenue Guy de Collongue, 69134 Ecully cedex, France

Received 9 November 2004, accepted after revision 20 September 2005

Available online 2 November 2005

Presented by Évariste Sanchez-Palencia

## Abstract

The transport of granular material often generates severe damage. Understanding the correlation between the friction coefficient, particle geometry and wear mechanisms is of primary importance for materials undergoing abrasive wear. The aim of this study is to investigate the effect of particle geometry on wear mechanisms and the friction coefficient. Numerical and analytical simulations and experimental results have been compared. The process to be studied is the scratch made by a rigid cone with different attack angles on a 5xxx aluminium alloy (Al–Mg) flat surface. A scratch test was used and the wear mechanisms were observed for different attack angles. A numerical study with a finite element code was made in order to understand the effect of attack angle on the friction coefficient. The contact surface and the friction coefficient were also studied, and the results compared to the Bowden and Tabor model. The superposition of the numerical, analytical and experimental results showed a better correlation between the wear mechanisms and the friction coefficient. It also showed the importance of the model hypothesis used to simulate the scratch phenomenon. *To cite this article: S. Mezlini et al., C. R. Mecanique 333 (2005).*

© 2005 Académie des sciences. Published by Elsevier SAS. All rights reserved.

## Résumé

**Étude expérimentale, numérique et analytique de l'usure abrasive : corrélation entre mécanismes d'usure et coefficient de frottement.** Le transport de matériaux granulaires génère souvent des endommagements sévères des surfaces avec lesquelles ils sont en contact. La compréhension de la corrélation entre le coefficient de frottement, la géométrie des particules et les mécanismes d'usure est très importante pour maîtriser l'usure abrasive. L'objectif de cette étude est d'étudier l'effet de la géométrie des particules sur les mécanismes d'usure et le coefficient de frottement lors d'un contact glissant sur une surface plane. Des simulations numériques et analytiques ont été comparées avec les résultats expérimentaux. Des essais de rayages ont été réalisés sur un alliage d'aluminium–magnésium du type 5xxx en utilisant des cônes rigides avec différentes géométries. Ce test permet de préciser l'effet de l'angle d'attaque sur les mécanismes d'usure. Un code de calcul par éléments finis est utilisé pour étudier l'effet de l'angle d'attaque sur le coefficient de frottement. La surface de contact et le coefficient de frottement ont été aussi étudiés et les résultats ont été comparés avec le modèle de Bowden et Tabor. La superposition des résultats numériques, analytiques et expérimentaux montre une bonne corrélation entre les mécanismes d'usure et le coefficient de frottement. L'importance des hypothèses du modèle utilisées pour simuler le phénomène de rayage a été aussi mise en évidence.

*Pour citer cet article : S. Mezlini et al., C. R. Mecanique 333 (2005).*

\* Corresponding author.

E-mail addresses: [salah.mezlini@ec-lyon.fr](mailto:salah.mezlini@ec-lyon.fr) (S. Mezlini), [tekaya\\_m@yahoo.fr](mailto:tekaya_m@yahoo.fr) (M. Ben Tkaya), [philippe.kapsa@ec-luon.fr](mailto:philippe.kapsa@ec-luon.fr) (Ph. Kapsa).

© 2005 Académie des sciences. Published by Elsevier SAS. All rights reserved.

**Keywords:** Friction; Wear; Abrasion; Analytical simulation; Numerical simulation

**Mots-clés :** Frottement ; Usure ; Abrasion ; Simulation analytique ; Simulation numérique

## 1. Introduction

When granular materials are transported, damage to the aluminium sheets used for the tipper of trucks, is observed. This degradation is caused by the sliding of the transported sand and gravel particles. When analysing this damage, caused in service, various morphologies and wear mechanisms corresponding to mild and severe abrasion are apparent. This damage is probably caused by the variation of loading conditions (pressure, sliding velocity and abrasive shape) during unloading of the granular material [1].

Most studies show that there are five fundamental wear modes: adhesive, tribochemical, fatigue, abrasive and erosive wear. Our study focuses on the abrasive wear mode, which can be expressed as the sum of three processes: cutting, ploughing and wedge formation [2]. In addition to the different operating conditions, such as normal load and sliding velocity, abrasive wear mechanisms are strongly related to the angularity of the abrasive particle [3–5].

Our study consists, on the one hand, in an experimental simulation of a rigid cone with different attack angles sliding against a 5xxx aluminium alloy sheet, and on the other hand, in a numerical and analytical simulation of a rigid cone sliding against a soft flat surface. By comparing the simulated and experimental results we were able to show the importance of the model hypothesis.

## 2. Experimentation

An aluminium alloy sheet is damaged by sliding, granular material. Scanning Electronic Microscopy (SEM) observations of the transported granular material show that the particles have different shapes (Fig. 1). We particularly distinguish two groups of particles: the first one contains gross particles, which have a rounded shape (Fig. 1(a)). The second group contains small particles with greater angularity (Fig. 1(b)). The particle's abrasiveness therefore changes from one particle to another, and the effect also depends on the orientation of the particle with respect to the contact surface. To simulate the effect of the particle geometry on abrasive wear mechanisms, rigid cones with different attack angle were used (Fig. 1).

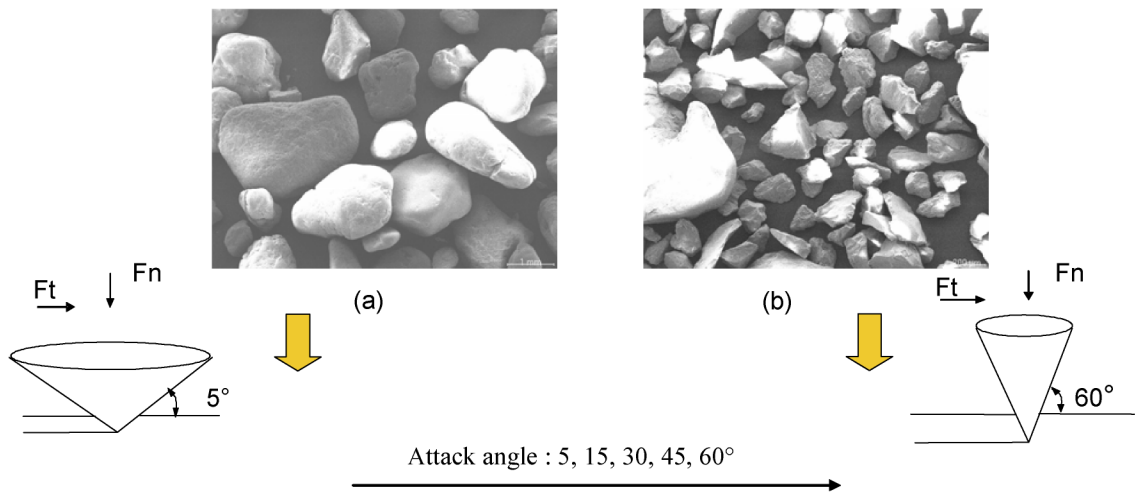


Fig. 1. SEM observations of transported granular material: (a) rounded particles, (b) sharp particles.

Fig. 1. Observations au MEB du matériau granulaire transporté : (a) particule ronde, (b) particule aiguë.

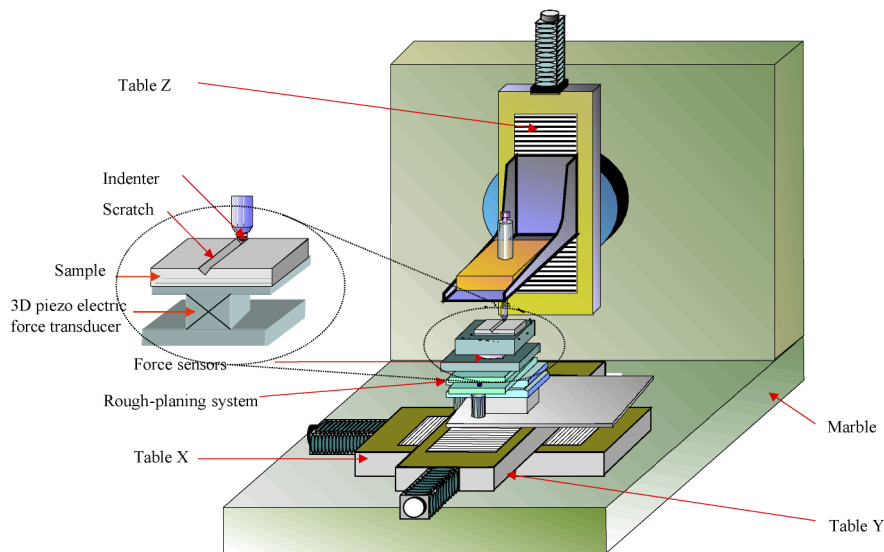


Fig. 2. Scratch tester.

Fig. 2. Test de rayage.

Table 1  
Experimental materials

Alloy designation (AFNOR)	Chemical composition (Weight %)	Condition	Vickers micro-hardness (Hv <sub>500g</sub> )
5xxx	Mg (3–4.5)	annealed	69

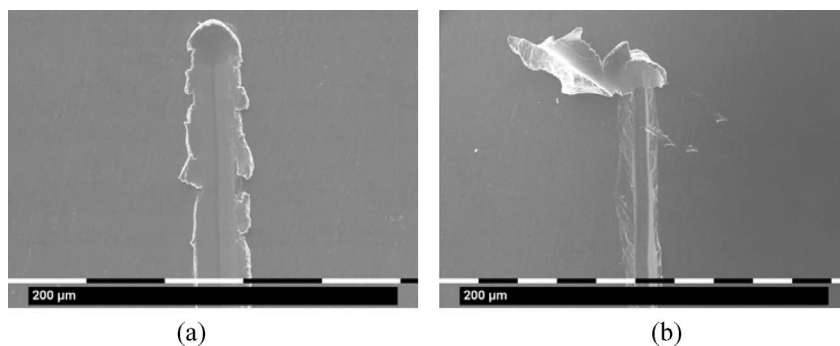


Fig. 3. SEM observations of aluminium alloy scratches for an attack angle: (a) 30° and (b) 60°.

Fig. 3. Observations au MEB des rayures sur des alliages d'aluminium pour des angles d'attaques : (a) 30° et (b) 60°.

For this, a scratch test was used (Fig. 2). This test, already described in [6], produces scratches using a rigid indenter. The sample surface is positioned so that it is parallel to the indenter motion by a specific, automatically controlled process.

To simulate the operating conditions, different attack angles, i.e. 5, 15, 30, 45 and 60 degrees, were selected. The normal load was set at 1 N. The scratch length and sliding velocity were set respectively at 3 mm and 250 µm/s.

Annealed 5xxx (Al–Mg) was tested. The properties of this alloy are detailed in Table 1.

For each test, the wear mechanisms were investigated using SEM observations. Figs. 3(a) and 3(b) show the wear mechanisms obtained by a conical indenter respectively for 30° and 60° attack angles. For the 30° attack angle, the material is pushed primarily to the side of the scratches, so a wedge is formed to the side and in front of the indenter. In this case, all the materials are pushed to the sides or to the front of the indenter without any loss of material. However,

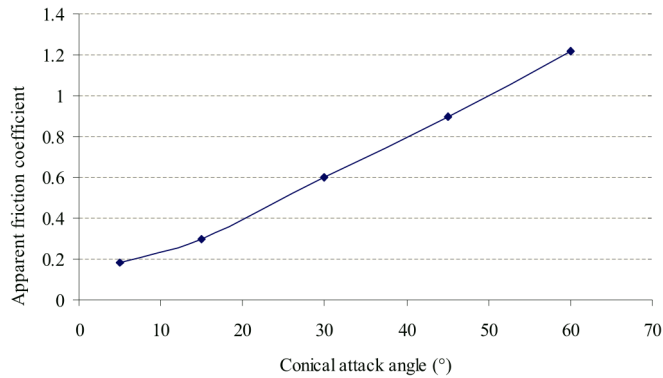


Fig. 4. Variation of experimental apparent friction coefficient with attack angle.

Fig. 4. Variation du coefficient de frottement expérimental apparent en fonction de l'angle d'attaque.

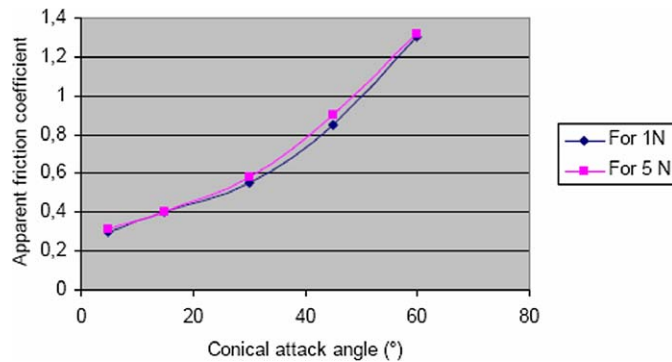


Fig. 5. Comparison between apparent friction coefficient for 1 and 5 N normal load against attack angle.

Fig. 5. Comparaison entre le coefficient de frottement en fonction de l'angle d'attaque pour l'effort normal de 1 et 5 N.

for the 60° attack angle, we have a transition of wear mechanisms from ploughing to cutting. Fig. 3(b) shows cutting mechanisms with the formation of chips in front of the indenter.

When analysing wear mechanisms in relation to different attack angles, three regions can be distinguished. When the attack angle is below 30°, a ploughing mechanism occurs whereas for an attack angle greater than 60°, a cutting mechanism dominates. For intermediate attack angles a transition from ploughing to cutting wear mechanism has been observed.

For each test, the apparent friction coefficient ( $\mu = F_t/F_n$ ) was also measured. Fig. 4 presents the variation of the mean apparent friction coefficient with the conical attack angle. It shows that the friction coefficient increases as the attack angle of the conical indenter increases. In fact, increasing the attack angle generates the transition of the wear mechanism from ploughing to cutting. This transition is accompanied by the severe plastic deformation necessary to generate a chip and damage the aluminium surface.

Similar results (friction coefficient and wear mechanisms) have been obtained for two normal loads, 1 and 5 N (Fig. 5).

### 3. Analytical modelling, scratch test, and comparisons with experimental results

Usually, scratch models consider ploughing and plastic behaviour for a simple shaped rigid indenter (cone, sphere or pyramid) in contact with a flat surface [7,8].

Here, we consider the model proposed by Bowden and Tabor [9]. This model was developed for a rigid conical indenter. It considers that the tangential force is split into two parts: the first one ( $F_p$ ) is necessary to plastically deform the material and the second one ( $F_a$ ) corresponds to the adhesion energy between the indenter and the material. The tangential force ( $F_t$ ) can then be expressed as:  $F_t = F_p + F_a$ .

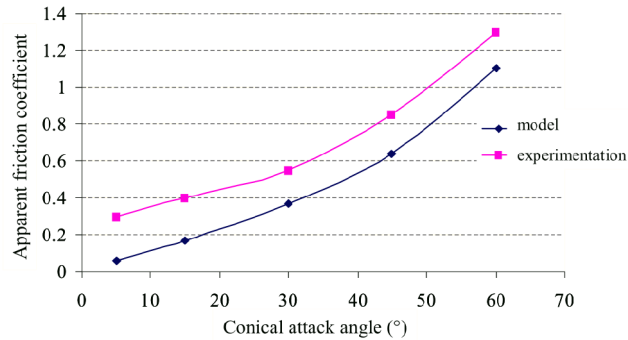


Fig. 6. Comparison between analytical and experimental apparent friction coefficients against attack angle.

Fig. 6. Comparaison entre le coefficient de frottement analytique et expérimental en fonction de l'angle d'attaque.

$F_p$  and  $F_a$  depend on the indenter's geometry, the material's properties and test conditions. Bowden and Tabor's model allows the apparent friction coefficient to be calculated by neglecting the adhesive component ( $F_a$ ). So the friction coefficient can be expressed as:  $\mu = F_t/F_N = F_p/F_N$ .

If the forces have been expressed with the flow pressure, the friction coefficient can be expressed as:  $\mu_0 = (A_p/A_s)(H_p/H_s)$ .

Here  $A_p$  and  $A_s$  are the surfaces of the contact projected in the normal and the tangential directions;  $H_p$  and  $H_s$  are the hardness in the normal and the tangential directions respectively.

If  $H_p = H_s$ , the apparent friction coefficient can be expressed as:  $\mu = (\frac{2}{\pi}) \cot \theta$  ( $\theta$  is the semi-angle of the tip).

Fig. 6 presents the comparison between experimental and analytical apparent friction coefficients obtained by the previous equation. It shows that the two curves have the same tendency and increase as the attack angle increases. However, the relative difference between experimental and analytical values is important for a small attack angle (attack angle less than  $30^\circ$ ). This phenomenon is probably caused by the absence of the adhesive component in the model. This result will be discussed in the following part.

In this Note the aim is to study the correlation between wear mechanisms and apparent friction coefficient. The correlation between hardness and wear resistance has been studied in a previous work [1].

#### 4. Numerical modelling scratch test

In this Note, the material's behaviour is modelled using large deformation and elastoplastic theory. More specifically, the plastic flow is described via the Von Mises plasticity criterion. The material's characteristics are representative of 5xxx aluminium alloy used to transport granular material, namely, a Young modulus of 70 GPa, a Poisson ratio of 0.3 and a constant yield stress  $\sigma_0$  of 140 MPa. A linear and non-linear elastic plastic behaviour have been used. It shows that the apparent friction coefficient depends slightly with the law behaviour. A rigid conical indenter was used to model the indenter.

The meshes are particularly refined near the indenter, but also are sufficiently large to approximate a semi-infinite solid [10,11] (Fig. 7). Loading is achieved by monitoring the indenter quasi-static displacement (dynamic effects are neglected), which is first pushed vertically into the volume to investigate the indentation, and then it is pushed horizontally to investigate the ploughing. Two models with and without remeshing have been used, respectively using ABAQUS/Explicit and ABAQUS/Standard. The same friction coefficient has been obtained for the two models.

The contact between the indenter and the surface is assumed to be a contact with local friction coefficient  $\mu_s$ .

The present study aims to better understand friction phenomena and particularly to correlate the friction coefficient to the geometry of the indenter and wear mechanisms. Many authors have studied the sliding contact of an asperity against a flat substrate [10,11]. They have also studied the effect of work hardening on a scratch test [12].

In this part, the correlation between indenter geometry (attack angle) and friction parameters, particularly the apparent friction coefficient, was studied. To study this phenomenon different attack angles (5, 15, 30, 45 and 60 degree) were selected. The contact between indenter and the surface is assumed to be frictionless. The results relating to a local friction coefficient  $\mu_s = 0.1$  are discussed.

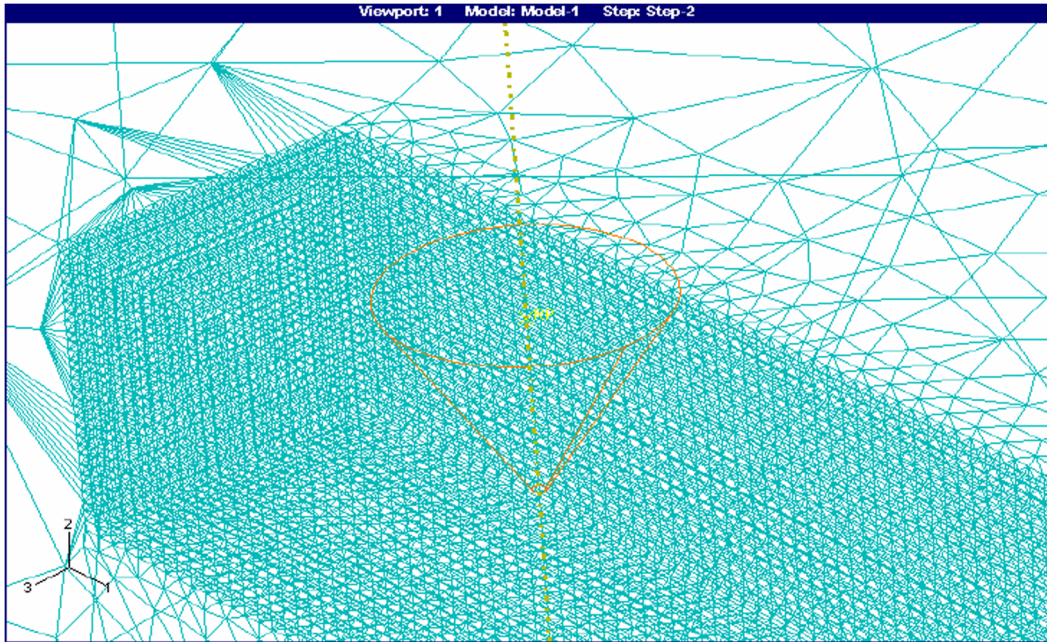


Fig. 7. Mesh used in numerical simulation.

Fig. 7. Maillage utilisé pour la simulation numérique.

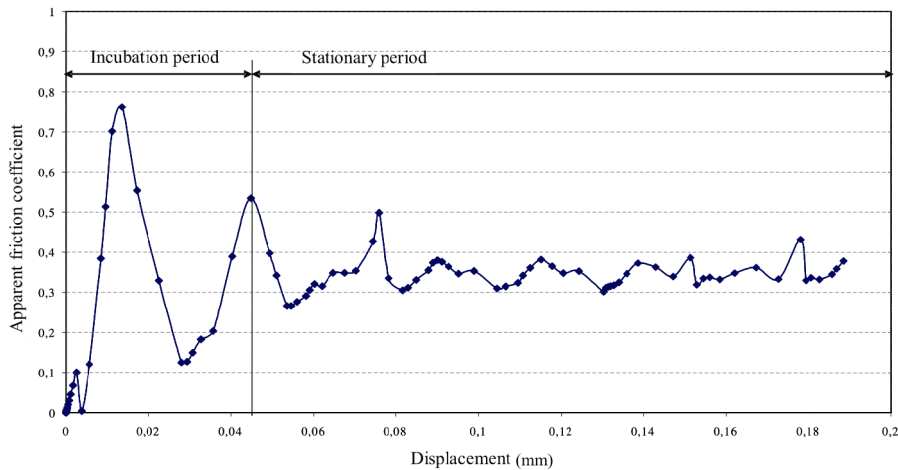


Fig. 8. Numerical apparent friction coefficient versus sliding distance for attack angle of 30°.

Fig. 8. Coefficient de frottement numérique apparent en fonction de la distance de glissement pour un angle d'attaque de 30°.

Fig. 8 shows the variation of the apparent friction coefficient versus the scratch length. It shows that there are two states: the first corresponds to an incubation period and the second one represents the stationary period when the friction coefficient remains constant. In this work, the average friction coefficient is calculated from the second state.

Fig. 9 represents the evolution of the friction coefficient versus the cone's attack angle. It also shows that the friction coefficient increases as the attack angle increases.

### 5. Comparison between experimental analytical and numerical modelling scratch test

In order to validate the analytical and numerical model, the experimental and modelled friction coefficients were compared. Fig. 10 shows the variation of the friction coefficient with the attack angle for the experimental, analytical

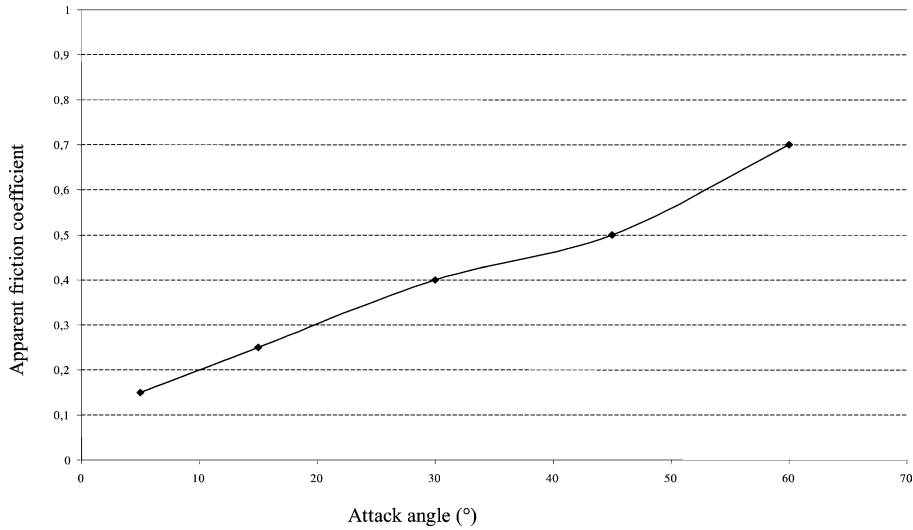


Fig. 9. Variation of numerical friction coefficient with attack angle.

Fig. 9. Variation du coefficient de frottement numérique en fonction de l'angle d'attaque.

*Variation du coefficient de frottement numérique en fonction de l'angle d'attaque.*

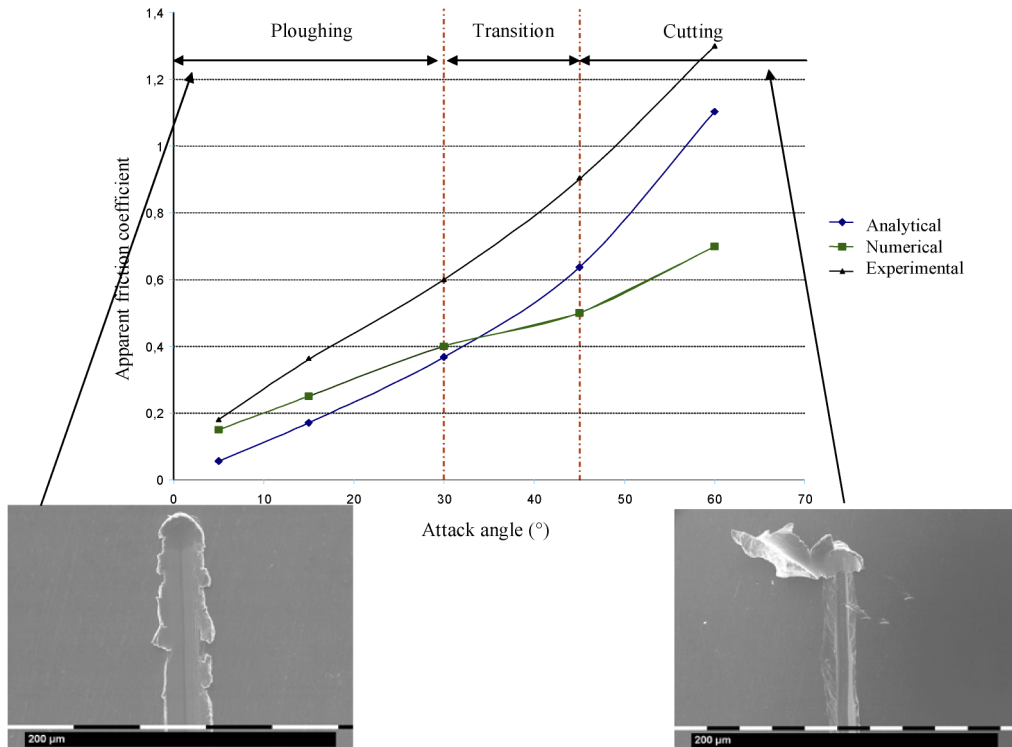


Fig. 10. Correlation between friction coefficient and wear mechanisms for different attack angle.

Fig. 10. Corrélation entre coefficient de frottement et mécanismes d'usure pour différent angle d'attaque.

and numerical simulations. It shows, in each case, that the friction coefficient increases as the attack angle increases. It also shows that for an attack angle below 30°, the numerical model correlates better with the experimental curve than the analytical model. This result is probably due to the absence of the adhesive component in the analytical model

( $F_a = 0$ ). However, for an attack angle over  $60^\circ$ , the analytical model correlates better with the experimental curve than the numerical model.

To explain this, wear mechanisms and the friction coefficient were correlated. For an attack angle below  $30^\circ$ , ploughing mechanism has been shown to occur (Fig. 10). Therefore, the adhesive component is not neglected and the Bowden and Tabor model hypothesis is not proven. However, the introduction of local friction coefficient ( $\mu_s = 0.1$ ) in the numerical model yielded better correlation with the experimental results.

For an attack angle over  $60^\circ$ , the cutting mechanism dominated. This mechanism requires severe plastic deformation to generate chips. So, the adhesive component can be neglected relative to that used to plastically deform the material and to generate chips. The analytical model hypothesis is proven, so the analytical model correlates better with the experimental results. For small attack angle wear mechanisms are similar to the one observed in experiments. However, for large attack angle differences in wear mechanisms between numerical and experimental analysis are observed. In experimental study and for a high attack angle, cutting wear mechanism with plastic deformation has been observed whereas, in numerical simulation only ploughing, wedge formation and plastic deformation have been occurred.

Another point is that, for the numerical model, we consider that there is no damage. This can explain the difference between experimental and numerical results obtained for wide attack angle. However, SEM observation contradicts this hypothesis and so limits the application of the numerical model for a wide attack angle (over  $60^\circ$ ).

## 6. Conclusions

In this Note, analytical and numerical simulations of the scratch phenomenon have been investigated. A scratch test was used to simulate the effect of particle geometry on damage to aluminium sheets. The experimental study was carried out to determine the friction coefficient and wear mechanisms for different attack angles. The variation of attack angle shows that there is a transition of wear mechanisms from ploughing for a small attack angle to cutting for a big attack angle.

A correlation between wear mechanism and friction coefficient has also been revealed. It shows that increasing the attack angle provokes both the transition of the wear mechanism from ploughing to cutting, and an increase of the friction coefficient.

A comparison between the experimental, analytical and experimental friction coefficient models shows that: for a small attack angle, the numerical model correlates better than the analytical model. This is due to the analytical model hypothesis, which neglects the adhesive effect. However, for a wide attack angle, the analytical model correlates better than the numerical model. This result is due to the neglect of the adhesive component in the cutting mechanism (and so the hypothesis of analytical model is proven). Moreover, in the numerical model, we consider that there is no damage. This consideration limits the numerical model's application when a wide attack angle is used. The numerical model can be improved by taking into account the damage phenomenon when the cutting mechanism occurs.

## References

- [1] S. Mezlini, Ph. Kapsa, C. Henon, J. Guilleminet, Abrasion of aluminium alloy: effect of subsurface hardness and scratch interaction simulation, *Wear* 257 (9–10) (2004) 892–900.
- [2] K. Kato, Micro-mechanisms of wear–wear modes, *Wear* 153 (1992) 277–295.
- [3] I.M. Hutchings, *Tribology: Friction and Wear of Engineering Materials*, Arnold, London, 1992.
- [4] S. Bahadur, R. Babruddin, Erodent particle characterization and the effect of particle size and shape on erosion, *Wear* 138 (1990) 189–208.
- [5] T. Sasada, M. Oike, N. Emori, The effect of abrasive grain size on the transition between abrasive and adhesive wear, *Wear* 97 (1984) 291–302.
- [6] V. Jardret, H. Zahouani, J.L. Loubet, T.G. Mathia, Understanding and quantification of elastic and plastic deformation during a scratch test, *Wear* 218 (1998) 8–14.
- [7] P. Gilormini, E. Felder, Theoretical and experimental study of ploughing of rigid-plastic semi-infinite body by a rigid pyramidal indenter, *Wear* 88 (1983) 195–206.
- [8] K. Komvopoulos, N. Saka, N.P. Suh, The mechanism of friction in boundary lubrication, *ASM J. Tribol.* 107 (1985) 452–462.
- [9] F.P. Bowden, D. Tabor, Friction, lubrication and wear: a survey of work during the last decade, *Brit. J. Appl. Phys.* 17 (1966) 1521–1544.
- [10] J.L. Bucaille, E. Felder, G. Hochstetter, *Wear* 249 (2001) 422–432.
- [11] M. Barge, P. Gilles et al., in: *Proceedings of the Euromech*, vol. 435, Valenciennes, France, June 2002, pp. 303–310.
- [12] M. Barge, G. Kermouche, P. Gilles, J.M. Bergheau, Experimental and numerical study of the ploughing part of abrasive wear, *Wear* 255 (2003) 30–37.